

# DOUBLE ATOMIC ELECTRON EMISSION FOLLOWING THE BETA DECAY OF ${}^6\text{He}$

Summary: Final charge-state distributions are calculated for the beta decay of  ${}^6\text{He}$  in a collaborative search for new physics beyond the Standard Model.



By **AARON BONDY** <bondy11u@uwindsor.ca> and **GORDON W. F. DRAKE** <gdrake@uwindsor.ca>

University of Windsor, Department of Physics, Essex Hall, 288-3 401 Sunset Avenue, Windsor, Ontario N9B 3P4

Aaron Bondy received 3<sup>rd</sup> place in the 2020 CAP Best Overall Student Oral Presentation

## INTRODUCTION

**B**eta decay has been a very interesting problem in the development of physics. From postulating the neutrino particle, to discovering the nonconservation of parity in the weak interaction, it has been centre stage in the arena of nuclear physics. In particular, in the early days of the electroweak theory, leading up to the Standard Model, beta decay was an important problem that was considered repeatedly ([1] and earlier references therein). A general  $\beta^-$  decay has the form

$$A(Z, N) \rightarrow A(Z + 1, N - 1) + e^- + \bar{\nu} \quad (1)$$

where  $Z$  is the nuclear charge and  $N$  is the number of neutrons. Two leptons (an electron and an antineutrino) are created, while a neutron changes to a proton. For single beta decay processes, there are two types, differing in how the product lepton spins couple in the aftermath of the decay:

1. Fermi V-type, where  $e^-$  and  $\bar{\nu}$  are coupled to form a total spin of 0; and
2. Gamow-Teller A-type where  $e^-$  and  $\bar{\nu}$  are coupled to form a total spin of 1.

The beta decay of  ${}^6\text{He}$  is predicted to be a pure Gamow-Teller process [2], which has an electron-neutrino correlation coefficient,  $a_{e\nu}$ , that is equal to  $-1/3$ , a quantity which under the present experimental conditions is related to the angle  $\theta$ , between  $e^-$  and  $\bar{\nu}$  (see Fig. 1) by

$$W(\theta) \propto 1 + a_{e\nu} \frac{v}{c} \cos \theta, \quad (2)$$

where  $W(\theta)$  describes the (measurable) angular distribution of observed electrons and  $\frac{v}{c}$  is the ratio between the speed of the electrons and the speed of light [3].

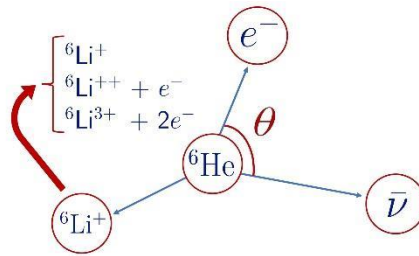


Figure 1. Kinematics of a  ${}^6\text{He}$  beta decay. The angle  $\theta$  between the electron and antineutrino is an important property used in testing the Standard Model. The daughter ion,  ${}^6\text{Li}^+$ , can undergo any excitation, single- or double-ionization process.

Since the antineutrino in this decay cannot be observed directly [4], it is necessary to reconstruct the kinematics using the momentum of the initial  ${}^6\text{He}$  atom, along with the other products (the beta particle and the recoiling daughter ion  ${}^6\text{Li}^+$ ). If in addition one or two atomic electrons boil off (shake-off) resulting in  ${}^6\text{Li}^{++}$  or  ${}^6\text{Li}^{3+}$ , this would affect the conservation of momentum and must thus be accounted for in deducing  $a_{ev}$ , the experimental quantity of interest.

Table I compares experimental results [1, 4] with our previous calculations [5] and earlier work by Wauters and Vaeck [6] for the probability of forming the various charge states  ${}^6\text{Li}^{k+}$ ,  $k = 1, 2, 3$  following beta decay from the ground  ${}^6\text{He}(1s^2\ ^1S)$  or metastable  ${}^6\text{He}(1s2s\ ^3S)$  states. Unless experiment and theory are brought into agreement for these probabilities, we cannot confidently interpret the experimental results to deduce  $a_{ev}$ . For both states shown in Table I, the probabilities for excitation (forming excited  ${}^6\text{Li}^+$ ) and single ionization ( ${}^6\text{Li}^{++}$ ) compare well. For double ionization ( ${}^6\text{Li}^{3+}$ ), though, there is a huge disagreement ( $\sim 2$  orders of magnitude) for both initial states. This discrepancy is what we seek to resolve in the present work.

TABLE I: Probabilities  $p({}^6\text{Li}^{k+})$  of forming the various charge states of  ${}^6\text{Li}^{k+}$ ,  $k = 1, 2, 3$  following beta decay of  ${}^6\text{He}(1s^2\ ^1S)$  or  ${}^6\text{He}(1s2s\ ^3S)$  as initial states. All quantities are expressed in percent (%).

Ion	Theory [5]	Theory [6]	Exp't. [1]
${}^6\text{He}(1s^2\ ^1S)$ initial state			
$p({}^6\text{Li}^+)$	89.03(3)	89.09	89.9(2)
$p({}^6\text{Li}^{++})$	9.7(1)	10.44	10.1(2)
$p({}^6\text{Li}^{3+})$	1.2(1)	0.32	0.018(15)
Total	99.9(1)	99.85	100.0(2)
${}^6\text{He}(1s2s\ ^3S)$ initial state			
$p({}^6\text{Li}^+)$	88.711(3)		89.9(3)(1)
$p({}^6\text{Li}^{++})$	9.42(7)		10.1(3)(1)
$p({}^6\text{Li}^{3+})$	1.86(7)		<0.01
Total	99.99(7)		100.00

## WAVE FUNCTIONS

Although the two-electron Schrödinger equation, with Hamiltonian (in atomic units),

$$H = -\frac{1}{2}\nabla_1^2 - \frac{1}{2}\nabla_2^2 - \frac{Z}{r_1} - \frac{Z}{r_2} + \frac{1}{r_{12}}, \quad (3)$$

is not exactly solvable, the solutions can be approximated by various methods including the Hartree-Fock and configuration-interaction methods. Our work employs the much more accurate (e.g. [8]) Hylleraas wave functions

$$\Psi(\mathbf{r}_1, \mathbf{r}_2) = \sum_{t=1}^2 \sum_{i,j,k} a_{ijk}^{(t)} r_1^i r_2^j r_{12}^k e^{-\alpha^{(t)} r_1 - \beta^{(t)} r_2} \times \mathcal{Y}_{l_1, l_2, L}^M \pm \text{exchange}, \quad (4)$$

that are essentially exact for bound states for all practical purposes, where  $\{a_{i,j,k}^{(t)}\}$  and  $\{\alpha^{(t)}, \beta^{(t)}\}$  are respectively the linear and nonlinear variational parameters. In Eq. 4,  $r_1 = \mathbf{r}_1$  and  $r_2 = \mathbf{r}_2$  are the radial positions of electrons 1 and 2,  $r_{12} = |\mathbf{r}_1 - \mathbf{r}_2|$  is the interelectronic distance, and  $\mathcal{Y}_{l_1, l_2, L}^M$  is the vector coupled spherical harmonic for a state with  $L, M$  quantum numbers. The eigenstates, called pseudostates, provide a discrete variational representation of the entire (bound + continuum) spectrum. Three important features of Hylleraas wave functions are that:

- They yield by far the most accurate wave functions for bound states.
- The discrete and complete basis set of pseudostates is computationally easier to deal with the infinity of Rydberg / continuum states.
- The pseudostates contain complete information about both the bound states and the scattering states, at least in the region of space near the nucleus.

The downside of the method is that each two-electron pseudostate represents an unresolved linear combination of both charge states  ${}^6\text{Li}^{++}$  and  ${}^6\text{Li}^{3+}$  for  $E > 0$ , as illustrated by the crosshatch pattern in Fig. 2 where the two scattering continua overlap.

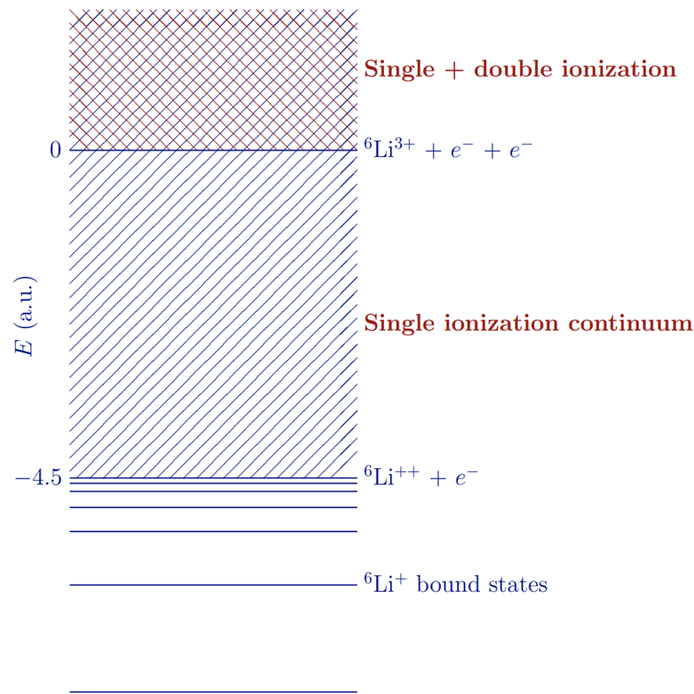


Figure 2. Energy level diagram for  ${}^6\text{Li}^+$  following beta decay. For  $E > 0$ , the single ionization continuum overlaps the double ionization continuum. This work seeks to resolve the fractional contribution from the two charge states.

## RESULTS

Our previous work [5] calculated the  ${}^6\text{Li}^+$  daughter ion probabilities using these Hylleraas wave functions and made use of the sudden approximation (SA), which assumes that the change in nuclear charge from  $Z = 2$  to  $Z = 3$ , due to the beta decay, is instantaneous. The SA is thought to be justified on the basis that the actual time taken for the change in nuclear charge is  $\sim 10^{-18}$  s, which is many orders of magnitude smaller than the relaxation time of the atomic electrons in the new Coulomb potential. Couratin *et al.* estimated that for the case of single-electron  ${}^6\text{He}^+$ , the SA alters the estimated that for the case of single-electron  ${}^6\text{He}^+$ , the SA alters the transition probabilities only at the 1% level [7].

According to the SA, the initial helium wave function  $\psi({}^6\text{He})$  is expanded in terms of the complete set of states  $\psi_n({}^6\text{Li}^+)$  according to

$$\Psi({}^6\text{He}) = \sum_n c_n \Psi_n({}^6\text{Li}^+). \quad (5)$$

The expansion coefficients,  $c_n$ , have the interpretation of probability amplitudes, and their squares, as probabilities in

$$p(E_n) = c_n^2 = |\langle \Psi({}^6\text{He}) | \Psi_n({}^6\text{Li}^+) \rangle|^2, \quad (6)$$

which gives the probability of transition to a daughter ion state with energy  $E_n$  following the decay. Our previous work partitioned the energy bins as indicated in Fig. 2, where (in a.u.)  $E_+ < -4.5$ ,  $-4.5 < E_{++} < 0$ , and  $E_{3+} > 0$  define bound, singly, and doubly ionized states, respectively. Although the first two energy bins unambiguously identify the charge state, the  $E > 0$  criterion could correspond to either single- or double-ionization, since one electron can feasibly be emitted with a large surplus of energy. This is the physical reason for the overlapping crosshatch region for  $E > 0$  in Fig. 2.

In order to remedy this problem, we have constructed projection operators that can be used to resolve the states with  $E > 0$  into  ${}^6\text{Li}^{++}$  or  ${}^6\text{Li}^{3+}$ , depending on whether single or double ionization boundary conditions are satisfied. To do this we took the following approach:

1. Form a complete set of one-electron pseudostates
2. Take their (anti)symmetrized products to form a complete set of two-electron pseudostates
3. Use these product states as the basis for a projection operator that will act on the  $\psi_n({}^6\text{Li}^+)$  Hylleraas eigenfunctions with  $E_n > 0$

The crucial part of the method is in step 2. In forming product states, we retain knowledge of what the charge state is of the two-electron system. This is because for each of the two one-electron states in step 1, the energy does unambiguously determine the charge state. However, in forming product states, we have neglected the electron-electron interaction, and hence have lost some information on the total energy. Fortunately, we have [9] accounted for this via perturbation corrections. We find that it is a completely negligible effect for present accuracy.

So, with two-electron wave functions that have well-defined boundary conditions in hand, we form the projection operator that will partition the previously overlapping  $E > 0$  region:

$$P = \sum_{n_{3+}} |n_{3+}\rangle \langle n_{3+}|, \quad (7)$$

where  $\{n_{3+}\}$  denotes those product wave functions corresponding to double ionization. Of course, we also have  $Q$ , formed as the sum of everything else, and satisfying  $P + Q = 1$ . The corrected probabilities (with  $p(E_n)$  from Eq. (6)) that we report are calculated as:

$$p^*(E_n) = \langle \Psi_n({}^6\text{Li}^+) | P | \Psi_n({}^6\text{Li}^+) \rangle \times p(E_n). \quad (8)$$

The finer details of our method have been omitted here (for the sake of brevity), but the interested reader can consult Ref. [9]. Our new results (in Table II) reduce the discrepancy between theory and experiment by an order of magnitude. Thus, there indeed was some  ${}^6\text{Li}^{++}$  masquerading as  ${}^6\text{Li}^{3+}$  in [5], as shown in Fig. 2; however, the  ${}^6\text{Li}^{3+}$  results still disagree by an order of magnitude for both starting states. This indicates that there is work left to be done on the problem.

TABLE II: Resolved  ${}^6\text{Li}^{3+}$  formation probabilities for each initial state following beta decay. All quantities are expressed in percent (%).

He state	$p({}^6\text{Li}^{3+})$		
	Theory [5]	Present work	Exp't [1, 4]
${}^6\text{He}(1s^2\ ^1S)$	1.2(1)	0.35(5)	0.018(15)
${}^6\text{He}(1s2s\ ^3S)$	1.86(7)	0.53(7)	<0.01
${}^6\text{He}(1s2s\ ^1S)$		0.56(6)	

## CONCLUSIONS

The projection operator formalism has reduced the discrepancy with experiment by almost an order of magnitude and, as developed, can be investigated for potential use in a range of atomic physics problems involving two electron continuum phenomena (e.g. double photoionization of He). Concerning the remaining discrepancy between theory and experiment (assuming that it is indeed on the theoretical side), one possibility would be to correct for the SA by solving the TDSE, where a time-dependent potential will be introduced in place of a step-function to model the beta particle.

## ACKNOWLEDGEMENTS

AB gratefully acknowledges funding from NSERC and QEII-GSST.

## REFERENCES

1. T. A. Carlson, F. Pleasonton, and C. H. Johnson, Electron shake off following the beta decay of  ${}^6\text{He}$ , *Phys. Rev.* **129**, 2220, (1963).
2. O. Naviliat-Cuncic and M. González-Alonso, Prospects for precision measurements in nuclear  $\beta$  decay in the LHC era, *Ann. Phys.* **525**, 600 (2013).
3. S. M. Wong, *Introductory nuclear physics*, Wiley and Sons, 1998.
4. R. Hong et al., Charge-state distribution of Li ions from the beta decay of laser-trapped  ${}^6\text{He}$  atoms, *Phys. Rev. A* **96**, 053411 (2017).
5. E. E. Schulhoff and G. W. F. Drake, Electron emission and recoil effects following the beta decay of  ${}^6\text{He}$ , *Phys. Rev. A* **92**, 050701 (2015).
6. L. Wauters and N. Vaeck, Study of the electronic rearrangement induced by nuclear transmutations: A B-spline approach applied to the beta decay of  ${}^6\text{He}$ , *Phys. Rev. C* **53**, 497, (1996).
7. C. Couratin et al., Measurement of the  ${}^6\text{Li}^+$  charge state distributions following the  ${}^6\text{He}$  beta decay, *J. Phys.: Conf. Series* **388**, 152013 (2012).
8. G. W. F. Drake, High precision theory of atomic helium, *Phys. Scr.* **T83**, 83 (1999).
9. A. T. Bondy and G. W. F. Drake, Charge state distributions after the beta decay of  ${}^6\text{He}$  to form  ${}^6\text{Li}^+$ , *Atoms* **11**, 41 (2023).